An inverse random source problem in a stochastic fractional diffusion equation

Pingping Niu*[1], Tapio Helin†[2], and Zhidong Zhang‡[2]

[1]School of Mathematical Sciences, Fudan University, China
[2]Department of Mathematics and Statistics, University of Helsinki, Finland

October 9, 2018

Abstract

In this work the authors consider an inverse source problem in the following stochastic fractional diffusion equation

$$\partial_t^\alpha u(x,t) + \mathcal{A}u(x,t) = f(x)h(t) + g(x)\dot{\mathbb{W}}(t).$$

The interested inverse problem is to reconstruct $f(x)$ and $g(x)$ by the statistics of the final time data $u(x,T)$. Some direct problem results are proved at first, such as the existence, uniqueness, representation and regularity of the solution. Then the reconstruction scheme for f and g is given. To tackle the ill-posedness, the Tikhonov regularization is adopted. Finally we give a regularized reconstruction algorithm and some numerical results are displayed.

Keywords: inverse problem, stochastic fractional diffusion equation, random source, Tikhonov regularization, reconstruction, regularity, partial measurements.

AMS subject classifications: 35R11, 35R30, 65C30, 65M32, 62N15.

1 Introduction

At a microscopic level, the physical phenomenon of diffusion is related to the random motion of individual particles. In one of his celebrated work, Einstein [13] deduced that the

*ppniu14@fudan.edu.cn
†tapio.helin@helsinki.fi
‡zhidong.zhang@helsinki.fi

density function of particles satisfies the classical diffusion equation under the key assumption that the mean squared displacement over a large number of jumps is proportional to time, i.e. $\overline{(\Delta x)^2} \propto t$. Currently, a large array of physical evidence suggests that there exists also physical diffusion that does not satisfy this assumption [27, 36, 9, 18]. In such *anomalous diffusion* the rate of mean squared displacement may satisfy $\overline{(\Delta x)^2} \propto t^\alpha$, $\alpha \neq 1$. The different rate introduces a modification to the diffusion equation in the form of time fractional derivative and the corresponding equations are often called fractional differential equations (FDEs). The applications of FDEs include, to name a few, the thermal diffusion in media with fractal geometry [38], highly heterogeneous aquifer [1], non-Fickian diffusion in geological formations [7], mathematical finance [6], underground environmental problem [20] and the analysis on viscoelasticity in material science [35, 46, 47].

Here we consider an FDE with a random source term

$$\begin{cases} \partial_t^\alpha u(x,t) + \mathcal{A}u(x,t) = F(x,t), & (x,t) \in D \times (0,T],\ \alpha \in (1/2,1); \\ u(x,t) = 0, & (x,t) \in \partial D \times (0,T]; \\ u(x,0) = 0, & x \in D, \end{cases} \tag{1.1}$$

where ∂_t^α is the Djrbashyan-Caputo fractional derivative given by the expression

$$\partial_t^\alpha u = \frac{1}{\Gamma(1-\alpha)} \int_0^t (t-\tau)^{-\alpha} u'(\tau)\, d\tau \quad \text{for} \quad 0 < \alpha < 1$$

and Γ stands for the Gamma function. However, we need a stricter restriction $\alpha \in (1/2, 1)$ on α for the regularity estimate, which can be seen in the proof of Lemma 3.4. Above, $D \subset \mathbb{R}^n$ is open and bounded, and the operator $\mathcal{A}$ with the definition

$$\mathcal{A}u = -\sum_{i,j=1}^n a^{ij}(x) u_{x_i x_j} + \sum_{i=1}^n b^i(x) u_{x_i} + c(x)u$$

with $a^{ij}, b^i, c \in C^\infty(\mathbb{R}^n)$ is symmetric, elliptic and positive definite. The random source term has the expression

$$F(x,y) = f(x)h(t) + g(x)\dot{\mathbb{W}}(t),$$

where the function $h \in L^\infty([0,T])$ is known and $\mathbb{W}$ is the standard Wiener process on a probability space $(\Omega, \mathcal{F}, \mathbb{P})$. Due to the randomness, we refer to (1.1) as stochastic fractional diffusion equation (SFDE) below. Let us point out that there are also other alternatives for the definition of the fractional derivative such as the Riemann–Liouville formulation, see [26, Chapter 2.1]. However, the Djrbashyan–Caputo derivative is often preferred due to its convenient properties related to boundary and initial conditions.

In this paper, we study the following inverse problem related to correlation based imaging:

given the empirical expectation and correlations of the final time data $u(x,T)$,
can we recover the unknown functions f and $|g|$?

Notice that the source term $g\dot{\mathbb{W}}$ has an invariant distribution with respect to the sign of g. Therefore, the recovery is considered up to the sign of g. We give a positive answer to this question and demonstrate it by numerical simulations.

Correlation based imaging has become common in applied inverse problems, where randomness is often an inherent part of the model. If the observational data is extensive but exceptionally corrupted or noisy, it can make more sense to analyze the correlations in the data that connect to the unknown parameters. This paradigm has interesting implications to the inverse problems research, since first, correlation-based imaging can remarkably reduce the ill-posedness of problems where no analytical solution is known (see [10]) and, second, it introduces a new set of analytical problems that need novel mathematical innovations [17, 22].

Our main contribution in this paper is to demonstrate that partial and noisy correlation data under different data acquisition geometries can yield useful information regarding the source terms f and g. We come to this conclusion as follows. We first give a construction of the solution to the stochastic direct problem and give suitable regularity estimates given different a priori smoothness of the source terms. Based on these results we show stability estimates for recovering f and $|g|$ (Theorem 4.2) and the uniqueness (Theorem 4.3) given infinite-precision correlation data of the final time solution $u(x, T)$. Meanwhile, the representation and the properties of Mittag–Leffler function introduced in section 2 yield mild ill-posedness for the inverse problem (Lemma 4.4). We demonstrate our results in practise with numerical simulations in section 5. We study different data acquisition geometries to find that satisfying localization of the sources can be achieved even if the observed subdomains are relatively small.

1.1 Outline of the paper

This paper is organized as follows. In section 2 we collect some preliminary material containing the properties of Mittag–Leffler function and the Itô isometry formula, which are crucial in the following proofs. Section 3 includes several results for the forward problem, which support the inverse problem work. We study the inverse problem in section 4, proving the stability, uniqueness and ill-posedness results. Finally, numerical demonstrations are given in section 5.

1.2 Previous literature

The fractional differential equations have drawn considerable amount of attention among mathematical community lately. Let us mention the work by Sakamoto and Yamamoto [43] to study the initial and boundary value problems for FDEs and the work by Luchko [33, 34] to establish the maximum principle in FDEs. Moreover, Jin, Lazarov and Zhou [24] gave a numerical scheme to approximate the FDE by the finite element method.

In terms of inverse problems, Cheng *et al* [11] gave one of the first proofs for a uniqueness theorem in one-dimensional FDE. The article [32] considered an inverse source problem in an FDE, which was close to this work. The authors in [31, 42] analyzed the distributed

differential equations, in which the assumption $\overline{(\Delta x)^2} \propto t^\alpha$ was extended to a more general case $\overline{(\Delta x)^2} \propto F(t)$, and studied some inverse problems in such equations. For an extensive review of the field we refer to [25] and references therein.

Time fractional stochastic PDEs have gained attention recently, see e.g. [14, 44, 37, 48] and references therein. Our setup differs slightly from these works: previous studies often assume some spatial randomness of the source, whereas our source term is random only in time. To accommodate the randomness in the spatial variable, one often smoothens the source in time. This operation is motivated and well explained in [37]. Let us also mention that first study of inverse source problems for time fractional stochastic PDEs were carried out in [45] for discrete random noise.

Correlation based imaging in inverse problems has been considered in applications already for a while, see e.g. the early work [12] on inverse random source problems. Since then correlation based imaging in random source problems has been considered widely in the framework of different PDE models by Li, Bao and others [30, 3, 28, 2, 5, 29, 4]. In this regard our paper provides the first study of random source problems in fractional diffusion models. Let us also point out that correlation based imaging has been considered for problems where the randomness is an inherent property of the medium or boundary condition [21, 22, 10, 17, 23, 16, 15, 8].

2 Preliminaries

Since $\mathcal{A}$ is a symmetric and elliptic operator with domain $L^2_0(D)$, then its eigensystem $\{(\lambda_n, \phi_n(x)) : n \in \mathbb{N}^+\}$ has the following properties: $0 < \lambda_1 \leq \lambda_2 \leq \cdots \leq \lambda_n < \cdots$ and $\{\phi_n : n \in \mathbb{N}^+\} \subset H^2(D) \cap H^1_0(D)$ constitutes an orthonormal basis of $L^2(D)$. Throughout the paper, we denote the inner product in $L^2(D)$ by $\langle \cdot, \cdot \rangle_{L^2(D)}$. Moreover, we write $f \lesssim g$ for two functions $f, g : X \to \mathbb{R}$ on some domain X if there is a universal constant $C > 0$ such that $f(x) \leq Cg(x)$ for all parameters $x \in X$. Similarly, we write $f \simeq g$ if both $f \lesssim g$ and $g \lesssim f$ hold.

Let us now introduce the Mittag–Leffler function which will play a central role in the following analysis. The Mittag–Leffler function is defined as

$$E_{\alpha,\beta}(z) = \sum_{k=0}^{\infty} \frac{z^k}{\Gamma(k\alpha + \beta)}$$

for $z \in \mathbb{C}$. Notice that this expression generalizes the natural exponential function since $E_{1,1}(z) = e^z$.

Let us next record some well-known properties of the function $E_{\alpha,\beta}$. Below, we study the behaviour of $E_{\alpha,\beta}$ only on the negative real line. However, the statements generalize to the complex plane. For reference, see [40, 26].

Lemma 2.1. *[40, Theorem 1.4] Let $0 < \alpha < 2$ and $\beta \in \mathbb{R}$ be arbitrary. Then it holds that*

$$|E_{\alpha,\beta}(-t)| \leq \frac{C}{1+t}$$

for any $t \geq 0$ and for any $p \in \mathbb{N}$ we have the asymptotic formula

$$E_{\alpha,\beta}(-t) = -\sum_{k=1}^{p} \frac{(-t)^{-k}}{\Gamma(\beta - \alpha k)} + \mathcal{O}(t^{-1-p})$$

as $t \to \infty$.

A useful result related to high order differentials of Mittag–Leffler functions is given by Sakamoto and Yamamoto in [43].

Lemma 2.2. *[43, Lemma 3.2] For $\lambda > 0,\ \alpha > 0$ and $n \in \mathbb{N}^+$, we have*

$$\frac{d^n}{dt^n} E_{\alpha,1}(-\lambda t^\alpha) = -\lambda t^{\alpha-n} E_{\alpha,\alpha-n+1}(-\lambda t^\alpha),\ t > 0.$$

A function $f : (0,\infty) \to \mathbb{R}$ is called *completely monotonic* if $f \in C^\infty(0,\infty)$ and

$$(-1)^n f^{(n)}(t) \geq 0$$

for all $t \in (0,\infty)$, i.e. the derivatives are alternating in sign. For the proof of the following result, see [41] and [19, Lemma 4.25].

Lemma 2.3. *For $0 < \alpha < 1$, functions $t \mapsto E_{\alpha,1}(-t)$ and $t \mapsto E_{\alpha,\alpha}(-t)$ are completely monotonic.*

Lemma 2.3 yields immediately the next corollary.

Corollary 2.4. *If $0 < \alpha < 1$ and $t > 0$, then $E_{\alpha,\alpha}(-t) \geq 0$.*

Finally, let us recall the well-known Itô isometry formula.

Lemma 2.5 ([39])**.** *Let $(\Omega, \mathcal{F}, \mathbb{P})$ be a probability space and let $f, g : [0,\infty) \times \Omega \to \mathbb{R}$ satisfy the following properties*

(1) $(t,\omega) \to f(t,\omega)$ is $\mathcal{B} \times \mathcal{F}$ -measurable, where $\mathcal{B}$ denotes the Borel σ-algebra on $[0,\infty)$;

(2) $f(t,\omega)$ is $\mathcal{F}_t$-adapted;

(3) $\mathbb{E} \int_S^T f^2(t,\omega) \mathrm{d}t < \infty$ for some $S, T > 0$.

Then it follows that

$$\mathbb{E}\left[\left(\int_S^T f(t,\omega)\ \mathrm{d}\mathbb{W}(t)\right)\left(\int_S^T g(t,\omega)\ \mathrm{d}\mathbb{W}(t)\right)\right] = \mathbb{E}\int_S^T f(t,\omega)g(t,\omega)\ \mathrm{d}t. \tag{2.1}$$

Later, we use the identity (2.1) for non-random functions and, consequently, the expectation on the right-hand side becomes trivial.

3 Direct problem

3.1 Solution to the SFDE (1.1)

Let us introduce the notion of mild solution for our stochastic fractional differential equation. To make sense of the solution, we need some assumptions regarding the source term.

Assumption 3.1. *We assume that $f, g \in L^2(D)$ such that $g \neq 0$ and $h \in L^\infty(0,T)$ is positive and bounded from below, i.e., there exists $c_h > 0$ s.t. $h \geq c_h$.*

Definition 3.2. *A stochastic process $u : [0,T] \times \Omega \to L^2(D)$ defined by*

$$u(\cdot, t, \omega) = \sum_{n=1}^{\infty} (I_{n,1}(t) + I_{n,2}(t,\omega))\phi_n(\cdot), \tag{3.1}$$

where

$$I_{n,1}(t) = f_n \int_0^t (t-\tau)^{\alpha-1} E_{\alpha,\alpha}(-\lambda_n (t-\tau)^\alpha) h(\tau)\, d\tau,$$
$$I_{n,2}(t,\omega) = g_n \int_0^t (t-\tau)^{\alpha-1} E_{\alpha,\alpha}(-\lambda_n (t-\tau)^\alpha)\, d\mathbb{W}(\tau),$$

with

$$f_n = \langle f(\cdot), \phi_n(\cdot)\rangle_{L^2(D)}, \;\; g_n = \langle g(\cdot), \phi_n(\cdot)\rangle_{L^2(D)},$$

is called a mild solution *of equation (1.1).*

The regularity of (3.1) is proved below in Lemma 3.4. Notice also that the term $I_{n,1}(t)$ is fully deterministic and contains only information regarding the deterministic part of the source. Similarly, the term $I_{n,2}$ carries the information related to the stochastic source. In the following, we omit the notation ω for brevity and make the connection to the random element implicit.

Remark 3.3. *The mild solutions to more general time-fractional stochastic PDEs have been considered in [44, 48] based on the semigroup approach taken in [14]. Our construction is related but uses the approach introduced by Sakamoto and Yamamoto in [43].*

Lemma 3.4. *The stochastic process u given in (3.1) satisfies*

$$\mathbb{E}\|u\|^2_{L^2(D\times[0,T])} \leq C\Big(\|h\|^2_{L^2(0,T)}\|f\|^2_{L^2(D)} + T^{2\alpha}\|g\|^2_{L^2(D)}\Big),$$

where $C > 0$ is a constant.

Proof. Recall that $\{\phi_n : n \in \mathbb{N}\}$ is an orthonormal basis of $L^2(D)$. Now for each $t \in [0,T]$ it holds that

$$\|u(\cdot,t)\|^2_{L^2(D)} = \left\|\sum_{n=1}^{\infty}(I_{n,1}(t) + I_{n,2}(t))\phi_n(\cdot)\right\|^2_{L^2(D)} = \sum_{n=1}^{\infty}(I_{n,1}(t) + I_{n,2}(t))^2$$
$$\leq 2\sum_{n=1}^{\infty}[I_{n,1}(t)]^2 + 2\sum_{n=1}^{\infty}[I_{n,2}(t)]^2.$$

Hence we have

$$\begin{aligned}
\mathbb{E}\|u\|^2_{L^2(D\times[0,T])} &= \mathbb{E}\left[\int_0^T \|u(\cdot,t)\|^2_{L^2(D)}\ dt\right] \\
&\lesssim \mathbb{E}\left[\int_0^T \sum_{n=1}^{\infty}[I_{n,1}(t)]^2 + \sum_{n=1}^{\infty}[I_{n,2}(t)]^2\ dt\right] \\
&= \int_0^T \sum_{n=1}^{\infty}[I_{n,1}(t)]^2\ dt + \mathbb{E}\left[\int_0^T \sum_{n=1}^{\infty}[I_{n,2}(t)]^2\ dt\right] \\
&= \sum_{n=1}^{\infty}\|I_{n,1}\|^2_{L^2(0,T)} + \int_0^T \sum_{n=1}^{\infty}\mathbb{E}I^2_{n,2}(t)\ dt \\
&:= S_1 + S_2.
\end{aligned}$$

First, consider the sum S_1. We can write the term $I_{n,1}$ as the convolution

$$I_{n,1}(t) = f_n(G_{\alpha,n} * h)(t)$$

where

$$G_{\alpha,n}(t) = t^{\alpha-1}E_{\alpha,\alpha}(-\lambda_n t^\alpha)$$

and, therefore, the Young's convolution inequality yields

$$\|I_{n,1}\|_{L^2(0,T)} \le f_n\|G_{\alpha,n}\|_{L^1(0,T)} \cdot \|h\|_{L^2(0,T)};$$

while the following result is derived from Lemmas 2.2, 2.3 and Corollary 2.4

$$\|G_{\alpha,n}\|_{L^1(0,T)} = \int_0^T t^{\alpha-1}E_{\alpha,\alpha}(-\lambda_n t^\alpha)dt = \frac{1 - E_{\alpha,1}(-\lambda_n T^\alpha)}{\lambda_n} \le \frac{1}{\lambda_1}.$$

In consequence, we can find the upper bound for S_1 as follows

$$S_1 \le \frac{1}{\lambda_1^2}\|h\|^2_{L^2(0,T)}\sum_{n=1}^{\infty} f_n^2 = C\|h\|^2_{L^2(0,T)}\|f\|^2_{L^2(D)}.$$

Second, let us consider S_2. For any $t \in [0,T]$ we have

$$\mathbb{E}I^2_{n,2}(t) = g_n^2\int_0^t \tau^{2\alpha-2}[E_{\alpha,\alpha}(-\lambda_n\tau^\alpha)]^2\ d\tau \le g_n^2\int_0^t \tau^{2\alpha-2}C^2\ d\tau = Cg_n^2 t^{2\alpha-1},$$

where we applied Lemmas 2.1, 2.5 and the restriction $\alpha \in (1/2, 1)$. Thus, the estimate of S_2 can be bounded by

$$S_2 \le \int_0^T \sum_{n=1}^{\infty} Cg_n^2 t^{2\alpha-1}\ dt = CT^{2\alpha}\sum_{n=1}^{\infty} g_n^2 \le CT^{2\alpha}\|g\|^2_{L^2(D)}.$$

Finally, combining the estimates for S_1 and S_2 yields the desired result. □

Lemma 3.4 considered the L^2 regularity of the solution over time and space. However, one can also study the space L^2-bound for u at a given time t.

Lemma 3.5. *The supremum of the expected norm of the solution satisfies*

$$\sup_{0\le t\le T}\mathbb{E}\left[\|u(\cdot,t)\|^2_{L^2(D)}\right]\le C\Big(\|h\|^2_{L^\infty[0,T]}\|f\|^2_{L^2(D)}+T^{2\alpha-1}\|g\|^2_{L^2(D)}\Big).$$

Moreover, if one has in addition that $g\in H^2(D)$, then

$$\sup_{0\le t\le T}\mathbb{E}\left[\|u(\cdot,t)\|^2_{H^2(D)}\right]\le C\Big(\|h\|^2_{L^\infty[0,T]}\|f\|^2_{L^2(D)}+T^{2\alpha-1}\|g\|^2_{H^2(D)}\Big).$$

Proof. From the proof of Lemma 3.4 we conclude that

$$\|u(\cdot,t)\|^2_{L^2(D)}\lesssim\sum_{n=1}^{\infty}[I_{n,1}(t)]^2+\sum_{n=1}^{\infty}[I_{n,2}(t)]^2$$

and

$$\|u(\cdot,t)\|^2_{H^2(D)}\simeq\|\mathcal{A}u(\cdot,t)\|^2_{L^2(D)}\lesssim\sum_{n=1}^{\infty}\lambda_n^2[I_{n,1}(t)]^2+\sum_{n=1}^{\infty}\lambda_n^2[I_{n,2}(t)]^2.$$

Similar to the proof of the previous lemma, we have

$$|I_{n,1}(t)|=|f_n(G_{\alpha,n}*h)(t)|\le|f_n|\cdot\|h\|_{L^\infty[0,T]}\int_0^t G_{\alpha,n}(\tau)d\tau\le\frac{1}{\lambda_n}|f_n|\cdot\|h\|_{L^\infty[0,T]}$$

and

$$\mathbb{E}I^2_{n,2}(t)\le Cg_n^2t^{2\alpha-1}.$$

Hence, we can deduce that

$$\begin{aligned}\sup_{0\le t\le T}\mathbb{E}\left[\|u(\cdot,t)\|^2_{L^2(D)}\right]&\lesssim\Big(\|h\|^2_{L^\infty[0,T]}\sum_{n=1}^{\infty}f_n^2+T^{2\alpha-1}\sum_{n=1}^{\infty}g_n^2\Big)\\&=\Big(\|h\|^2_{L^\infty[0,T]}\|f\|^2_{L^2(D)}+T^{2\alpha-1}\|g\|^2_{L^2(D)}\Big)\end{aligned}$$

and

$$\begin{aligned}\sup_{0\le t\le T}\mathbb{E}\left[\|u(\cdot,t)\|^2_{H^2(D)}\right]&\lesssim\Big(\|h\|^2_{L^\infty[0,T]}\sum_{n=1}^{\infty}f_n^2+T^{2\alpha-1}\sum_{n=1}^{\infty}\lambda_n^2g_n^2\Big)\\&\lesssim\Big(\|h\|^2_{L^\infty[0,T]}\|f\|^2_{L^2(D)}+T^{2\alpha-1}\|g\|^2_{H^2(D)}\Big).\end{aligned}$$

This completes the proof. □

4 Reconstruction of f and $|g|$ from the final time correlations

In this section we consider the inverse problem of reconstructing f and $|g|$. Let $X, Y : \Omega \to \mathbb{R}$ be random variables on some complete probability space. Below, we write $\mathbb{V}(X) := \mathbb{E}(X - \mathbb{E}X)^2$ and

$$\mathrm{Cov}(X, Y) := \mathbb{E}(X - \mathbb{E}X)(Y - \mathbb{E}Y)$$

for the variance and covariance, respectively. We assume that our data is partial information regarding the distributions of random variables $u_n(T)$ defined by

$$u_n(T) := \langle u(\cdot, T), \phi_n(\cdot) \rangle_{L^2(D)}$$

for any $n \in \mathbb{N}^+$.

4.1 Stability of the reconstruction

From Definition 3.2 and Lemma 2.5 it follows that the final time expectation and variance can be formulated as

$$\begin{aligned} \mathbb{E}u_n(T) &= f_n \int_0^T \tau^{\alpha-1} E_{\alpha,\alpha}(-\lambda_n \tau^\alpha) h(T-\tau)\, d\tau, \\ \mathbb{V}(u_n(T)) &= g_n^2 \int_0^T \tau^{2\alpha-2} [E_{\alpha,\alpha}(-\lambda_n \tau^\alpha)]^2\, d\tau \end{aligned} \tag{4.1}$$

for any $n \in \mathbb{N}^+$. To show the stability result, we deduce the coming lemma at first.

Lemma 4.1. *For each $n \in \mathbb{N}^+$, there exists a constant $C > 0$ independent of n such that*

$$\left| \int_0^T \tau^{\alpha-1} E_{\alpha,\alpha}(-\lambda_n \tau^\alpha) h(T-\tau)\, d\tau \right| \geq C\lambda_n^{-1}$$

and

$$\left| \int_0^T \tau^{2\alpha-2} [E_{\alpha,\alpha}(-\lambda_n \tau^\alpha)]^2\, d\tau \right| \geq C\lambda_n^{-2}.$$

Proof. For the first estimate, by Lemma 2.2 and Assumption 3.1, we obtain

$$\begin{aligned} \left| \int_0^T \tau^{\alpha-1} E_{\alpha,\alpha}(-\lambda_n \tau^\alpha) h(T-\tau)\, d\tau \right| &\geq c_h \int_0^T \tau^{\alpha-1} E_{\alpha,\alpha}(-\lambda_n \tau^\alpha)\, d\tau \\ &= c_h \lambda_n^{-1} [1 - E_{\alpha,1}(-\lambda_n T^\alpha)] \\ &\geq c_h \lambda_n^{-1} [1 - E_{\alpha,1}(-\lambda_1 T^\alpha)] \\ &\gtrsim \lambda_n^{-1}. \end{aligned}$$

For the second one, Lemmas 2.1 and 2.2 yield

$$\begin{aligned}\left|\int_0^T \tau^{2\alpha-2}[E_{\alpha,\alpha}(-\lambda_n\tau^\alpha)]^2\ d\tau\right| &\geq [E_{\alpha,\alpha}(-\lambda_n T^\alpha)]^2 \int_0^T \tau^{2\alpha-2}\ d\tau \\ &\gtrsim T^{2\alpha-1}\lambda_n^{-2}T^{-2\alpha} \\ &\gtrsim \lambda_n^{-2}\end{aligned}$$

and complete the proof. □

Now a stability result follows in a straightforward manner.

Theorem 4.2 (Stability)**.** *Suppose Assumption 3.1 is satisfied and, in addition, $g \in H^2(D)$. Then there exists a constant $C > 0$ such that*

$$\|f\|^2_{L^2(D)} + \|g\|^2_{L^2(D)} \leq C\mathbb{E}\|u(\cdot,T)\|^2_{H^2(D)}.$$

Proof. Lemma 4.1 and the Jensen inequality yield that

$$f_n^2 + g_n^2 \lesssim \lambda_n^2\left((\mathbb{E}u_n(T))^2 + \mathbb{V}(u_n(T))\right) = \lambda_n^2\mathbb{E}(u_n(T))^2.$$

Therefore, it follows that

$$\|f\|^2_{L^2(D)} + \|g\|^2_{L^2(D)} = \sum_{n=1}^{\infty}(f_n^2+g_n^2) \lesssim \sum_{n=1}^{\infty}\lambda_n^2\mathbb{E}(u_n(T))^2 \lesssim \mathbb{E}\|u(\cdot,T)\|^2_{H^2(D)}.$$

The proof is complete. □

4.2 Uniqueness of the reconstruction

As discussed above, the stochastic FDE in (1.1) is invariant with respect to the sign of g. Therefore, the observations of the final time do not contain information regarding the sign. However, notice carefully that the observed expectation and variance do not ensure uniqueness for $|g|$, since each process $\langle u, \phi_n\rangle_{L^2(D)}$ is invariant to the sign of g_n independently. As we will see below, the cross-covariance between $u_n(T)$ and $u_k(T)$ for $k \neq n$ adds the crucial information to the system since the random white noise in (1.1) is only time-dependent.

By our Definition 3.2 and Lemma 2.5, the covariance $\mathrm{Cov}(u_m(T), u_n(T))$ is given by identity

$$\mathrm{Cov}(u_m(T), u_n(T)) = g_m g_n \int_0^T \tau^{2\alpha-2}E_{\alpha,\alpha}(-\lambda_m\tau^\alpha)E_{\alpha,\alpha}(-\lambda_n\tau^\alpha)\ d\tau \tag{4.2}$$

for any $m, n \in \mathbb{N}^+$. A uniqueness result can now be provided as follows.

Theorem 4.3 (Uniqueness). *Suppose Assumption 3.1 holds and $g \in H^2(D)$. Moreover, let N_0 be an index such that $\langle g, \phi_{N_0}\rangle_{L^2(D)} \neq 0$. The expectation of the final time solution and the correlations at N_0, i.e. the quantities*

$$\left\{\mathbb{E}[u_n(T)], \mathbb{V}(u_{N_0}(T)), \mathrm{Cov}(u_{N_0}(T), u_n(T)) \ : \ n \in \mathbb{N}^+\right\}$$

determine the source terms f and $|g|$ uniquely.

Proof. First, we clearly have

$$f_n = \frac{\mathbb{E}u_n(T)}{\int_0^T \tau^{\alpha-1} E_{\alpha,\alpha}(-\lambda_n \tau^\alpha) h(T-\tau)\ d\tau},$$

which is well-defined due to Assumption 3.1.

Second, due to the assumption on N_0, the variance $\mathbb{V}(u_{N_0}(T))$ yields $|g_{N_0}|$ up to the sign from equation (4.1). For convenience, we pick the positive solution of g_{N_0}. It follows that

$$g_n = \frac{\mathrm{Cov}(u_{N_0}(T), u_n(T))}{g_{N_0} \int_0^T \tau^{2\alpha-2} E_{\alpha,\alpha}(-\lambda_{N_0}\tau^\alpha) E_{\alpha,\alpha}(-\lambda_n \tau^\alpha)\ d\tau}.$$

The integral in the denominator is strictly positive due to $g_{N_0} > 0$. □

Ill-posedness of the recovery can be characterized by the following lemma.

Lemma 4.4. *There exists a constant C which is independent of n such that*

$$\left| \int_0^T \tau^{\alpha-1} E_{\alpha,\alpha}(-\lambda_n \tau^\alpha) h(T-\tau)\ d\tau \right| \leq C\lambda_n^{-1}$$

and

$$\left| \int_0^T \tau^{2\alpha-2} E_{\alpha,\alpha}(-\lambda_{N_0}\tau^\alpha) E_{\alpha,\alpha}(-\lambda_n \tau^\alpha)\ d\tau \right| \leq C\lambda_n^{-1+\frac{1}{2\alpha}}.$$

Proof. Lemma 2.2 implies that

$$\begin{aligned} \left| \int_0^T \tau^{\alpha-1} E_{\alpha,\alpha}(-\lambda_n \tau^\alpha) h(T-\tau)\ d\tau \right| &\leq \|h\|_{L^\infty(0,T)} \int_0^T \tau^{\alpha-1} E_{\alpha,\alpha}(-\lambda_n \tau^\alpha)\ d\tau \\ &= \|h\|_{L^\infty(0,T)} \lambda_n^{-1}(1 - E_{\alpha,1}(-\lambda_n T^\alpha)) \\ &\lesssim \lambda_n^{-1}. \end{aligned}$$

On the other hand, if we let

$$t_* = \lambda_n^{-\frac{1}{2\alpha}} \tag{4.3}$$

and use Lemma 2.1 to obtain

$$E_{\alpha,\alpha}(-\lambda_n t^\alpha) \leq \begin{cases} C & \text{for } t < t_* \text{ and} \\ \frac{C}{\lambda_n t^\alpha} & \text{for } t \geq t_*, \end{cases}$$

then it follows that

$$\begin{aligned}
&\left| \int_0^T \tau^{2\alpha-2} E_{\alpha,\alpha}(-\lambda_{N_0}\tau^\alpha) E_{\alpha,\alpha}(-\lambda_n \tau^\alpha)\, d\tau \right| \\
&\qquad = \int_0^{t_*} \tau^{2\alpha-2} E_{\alpha,\alpha}(-\lambda_{N_0}\tau^\alpha) E_{\alpha,\alpha}(-\lambda_n \tau^\alpha)\, d\tau \\
&\qquad\quad + \int_{t_*}^T \tau^{2\alpha-2} E_{\alpha,\alpha}(-\lambda_{N_0}\tau^\alpha) E_{\alpha,\alpha}(-\lambda_n \tau^\alpha)\, d\tau \\
&\qquad \le \int_0^{t_*} \tau^{2\alpha-2} C^2\, d\tau + \int_{t_*}^T \tau^{2\alpha-2} C\tau^{-\alpha} (\lambda_n \tau^\alpha)^{-1}\, d\tau \\
&\qquad \lesssim t_*^{2\alpha-1} + \lambda_n^{-1} t_*^{-1} - \lambda_n^{-1} T^{-1} \\
&\qquad \lesssim \lambda_n^{-1+\frac{1}{2\alpha}}.
\end{aligned}$$

Above, we find that the choice in (4.3) optimizes the rate. This completes the proof. □

5 Numerical reconstruction

In this section we illustrate the practical solvability of the inverse problem by numerical demonstrations. We consider to reconstruct f and $|g|$ in the finite dimensional space

$$\mathcal{S}_N := \mathrm{Span}\{\phi_n : 1 \le n \le N\},$$

where ϕ_n are the eigenfunctions of $\mathcal{A}$, and denote the approximations of f and g as

$$f_N(x) = \sum_{n=1}^N f_n \phi_n(x), \quad g_N(x) = \sum_{n=1}^N g_n \phi_n(x).$$

Also the vector formulations of f_N and g_N can be given as

$$\vec{f}_N = \begin{bmatrix} f_1 & f_2 & \cdots & f_N \end{bmatrix}, \quad \vec{g}_N = \begin{bmatrix} g_1 & g_2 & \cdots & g_N \end{bmatrix}.$$

The domain D is set to be the unit circle in $\mathbb{R}^2$ and we let $\mathcal{A} = -\Delta$, then it follows that the eigenfunctions of $\mathcal{A}$ are given by

$$\phi_n(r,\theta) = w_n J_m(\sqrt{\lambda_n} r) \cos(m\theta + d_n),$$

where (r,θ) are the polar coordinates on D, the phase d_n is either 0 or $\pi/2$, w_n is the normalized weight factor and $J_m(z)$ is the first kind Bessel function with degree m. The eigenvalues $\{\lambda_n : n \in \mathbb{N}^+\}$ are the squares of the zeros of the class of Bessel functions $\{J_m(z) : m \in \mathbb{N}\}$ and indexed by n with nondecreasing order. Hence, we can see the index m is a function of n, i.e. $m = m(n)$. The set $\{\lambda_n : n \in \mathbb{N}^+\}$ can be solved numerically and satisfy $\lambda_j \simeq j^2$. The data used in all examples below is simulated and the forward

solver being used is based on a finite difference scheme. We run the forward solver 10^3 times for different realizations of the source term and average the final time data $u(x,T)$ to get the approximatively exact data $\widehat{\mathbf{E}}, \widehat{\mathbf{C}}$. Lastly, we generate the noisy data $\widehat{\mathbf{E}}^\delta, \widehat{\mathbf{C}}^\delta$ for all examples by adding 1% relative noise.

We consider the two experiments $(e1)$ and $(e2)$, where we use the following source terms:

$$\begin{aligned}
(e1): \quad f(r,\theta) =& 10w_1 J_{m(1)}(\sqrt{\lambda_1}r)\cos(m(1)\theta) + 5w_2 J_{m(2)}(\sqrt{\lambda_2}r)\cos(m(2)\theta) \\
&+ 12w_2 J_{m(2)}(\sqrt{\lambda_2}r)\sin(m(2)\theta), \\
g(r,\theta) =& 10w_1 J_{m(1)}(\sqrt{\lambda_1}r)\cos(m(1)\theta) + 2w_2 J_{m(2)}(\sqrt{\lambda_2}r)\cos(m(2)\theta) \\
&+ 13w_2 J_{m(2)}(\sqrt{\lambda_2}r)\sin(m(2)\theta); \\
(e2): \quad f(x,y) =& 6\chi_{[(x-0.3)^2+0.5(y-0.2)^2<0.2^2]}, \\
g(x,y) =& -3\chi_{[0.3(x+0.4)^2+(y+0.3)^2<0.15^2]}.
\end{aligned}$$

The source terms in $(e1)$ and $(e2)$ are represented in Figure 1.

5.1 Data acquisition and finite-dimensional data

In practise, the data acquisition is unlikely to happen in the basis ϕ_n indicated by $\mathcal{A}$. For example, the fact that functions ϕ_n are not local can be restrictive, if the observations are limited to a strict subset $D_{mea} \subset D$. To accommodate this thought, suppose our data is given on the basis functions of a finite dimensional subspace $\widehat{\mathcal{S}}_K \subset L^2(D)$ such that

$$\widehat{\mathcal{S}}_K = \mathrm{Span}\{\psi_n(x) : n = 1, ..., K\},$$

and our data is given by

$$\{\mathbb{E}\widehat{u}_n(T), \mathrm{Cov}(\widehat{u}_k(T), \widehat{u}_\ell(T)) \ : \ k \in \mathcal{I}, \ell \in \mathcal{J} \text{ and } n \in \mathcal{I} \cup \mathcal{J}\}$$

where $\widehat{u}_n(T) = \langle u(T), \psi_n \rangle_{L^2(D)}$ and $\mathcal{I}, \mathcal{J} \subset \{1, ..., K\}$ are some index subsets. For convenience, we assume that $\mathcal{I} = \mathcal{J} = \{1, ..., K\}$ and, therefore, omit denoting the dependence on the index sets.

Source-to-expectation mapping. Writing $\mathbb{E}\widehat{u}_n(T)$ in the $\{\phi_k\}_{k=1}^\infty$ basis yields

$$\begin{aligned}
\mathbb{E}\widehat{u}_n(T) &= \sum_{k=1}^\infty \langle \psi_n, \phi_k \rangle \mathbb{E}\langle u(T), \phi_k \rangle \\
&= \sum_{k=1}^\infty \langle \psi_n, \phi_k \rangle \cdot f_k \int_0^T \tau^{\alpha-1} E_{\alpha,\alpha}(-\lambda_k \tau^\alpha) h(T-\tau)\, d\tau.
\end{aligned}$$

Therefore, by using notation $\widehat{\mathbf{E}} = (\mathbb{E}\widehat{u}_n(T))_{n=1}^K \in \mathbb{R}^K$, we have identity

$$\widehat{\mathbf{E}} = Af,$$

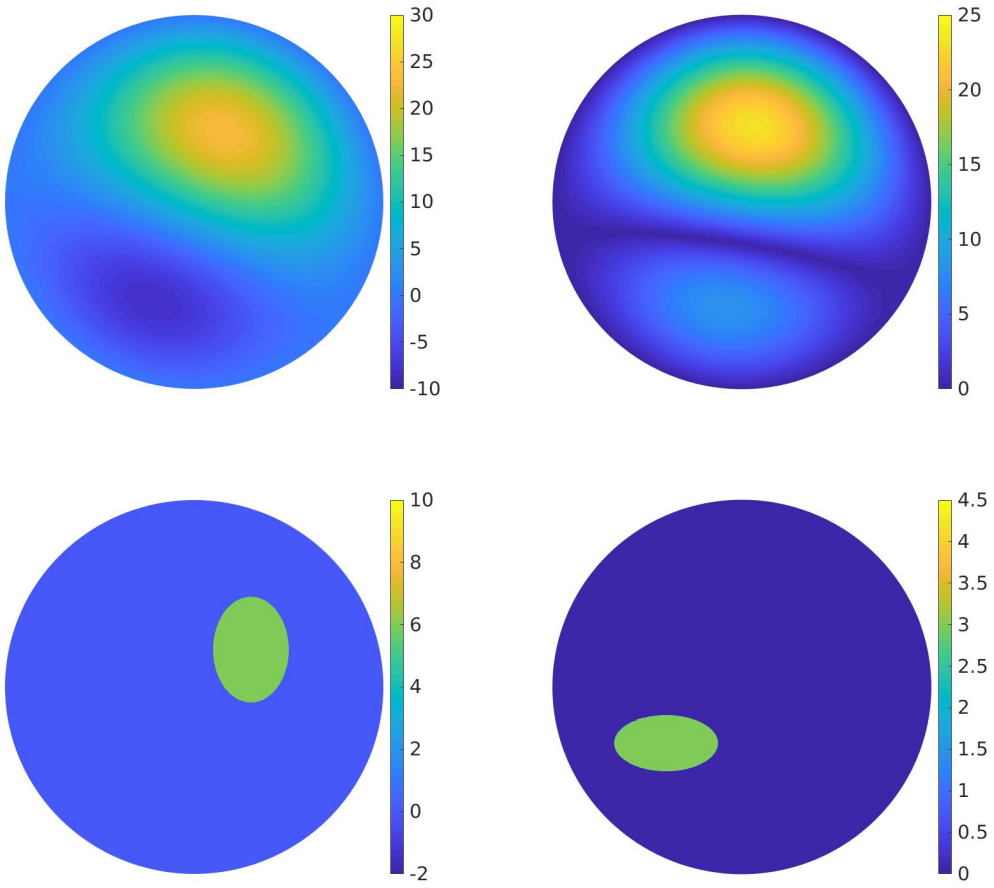

Figure 1: Exact solutions of $(e1)$ (top) and $(e2)$ (bottom): f (left), $|g|$ (right).

where the operator $A : L^2(D) \to \mathbb{R}^N$ is linear and bounded due to Lemma 3.5 and satisfies

$$(Af)_n = \langle z_n, f \rangle$$

with

$$z_n = \sum_{k=1}^{\infty} \int_0^T \tau^{\alpha-1} E_{\alpha,\alpha}(-\lambda_k \tau^\alpha) h(T-\tau)\, d\tau \cdot \langle \psi_n, \phi_k \rangle \phi_k.$$

Source-to-covariance mapping. We see that we have

$$\begin{aligned} \mathrm{Cov}(\widehat{u}_m(T), \widehat{u}_n(T)) &= \sum_{k=1}^{\infty} \sum_{\ell=1}^{\infty} \mathrm{Cov}(u_k, u_\ell) \langle \psi_m, \phi_k \rangle \langle \psi_n, \phi_\ell \rangle \\ &= \boldsymbol{\psi}_m^\top \mathbf{C} \boldsymbol{\psi}_n, \end{aligned}$$

where $\boldsymbol{\psi}_m = (\langle \psi_m, \phi_k \rangle)_{k=1}^{\infty}$ and $\mathbf{C} = (\mathrm{Cov}(u_k, u_\ell))_{k,\ell=1}^{\infty}$. By writing $\mathbf{R} = (\boldsymbol{\psi}_1, ..., \boldsymbol{\psi}_K)$, we see

$$\widehat{\mathbf{C}} = \mathbf{R}^\top \mathbf{C} \mathbf{R}.$$

Recall now the expression for $\mathrm{Cov}(u_m(T), u_n(T))$ in (4.2). We can rewrite (4.2) in the form

$$\mathbf{C} = \int_0^T \mathbf{g}(\tau)\mathbf{g}(\tau)^\top d\tau,$$

where

$$\mathbf{g}(\tau) = \left(g_k \tau^{\alpha-1} E_{\alpha,\alpha}(-\lambda_k \tau^\alpha)\right)_{k=1}^{\infty} : [0,T] \to \mathbb{R}^\infty.$$

In consequence, we have

$$\widehat{\mathbf{C}} = \int_0^T \mathbf{R}^\top \mathbf{g}(\tau)\mathbf{g}(\tau)^\top \mathbf{R}\, d\tau. \tag{5.1}$$

Let us consider now the integrand in (5.1). We obtain

$$\begin{aligned}
(\mathbf{R}^\top \mathbf{g}(\tau))_m &= \boldsymbol{\psi}_m \cdot \mathbf{g}(\tau) \\
&= \sum_{k=1}^{\infty} \langle \psi_m, \phi_k \rangle \langle g, \phi_k \rangle \tau^{\alpha-1} E_{\alpha,\alpha}(-\lambda_k \tau^\alpha) \\
&= \left\langle g, \sum_{k=1}^{\infty} \langle \psi_m, \phi_k \rangle \tau^{\alpha-1} E_{\alpha,\alpha}(-\lambda_k \tau^\alpha) \phi_k \right\rangle \\
&= \langle g, w_m(\tau) \rangle
\end{aligned}$$

where

$$w_m(\tau) = \sum_{k=1}^{\infty} \langle \psi_m, \phi_k \rangle \tau^{\alpha-1} E_{\alpha,\alpha}(-\lambda_k \tau^\alpha) \phi_k.$$

Let us define an operator $B : H^2(D) \to \mathbb{R}^{K \times K}$ by

$$Bg = \int_0^T \mathbf{R}^\top \mathbf{g}(\tau)\mathbf{g}(\tau)^\top \mathbf{R}\, d\tau. \tag{5.2}$$

Clearly, due to Lemma 3.5 the operator B is bounded. Now we can state the discretized equations for f and g:

$$Af = \widehat{\mathbf{E}} \quad \text{and} \quad Bg = \widehat{\mathbf{C}}.$$

5.2 Numerical results with observations on the full domain

Here we investigate the numerical reconstruction with observations on the full domain, i.e. $D_{mea} = D$, but with correlations based on one fixed point. In other words, we assume that $\{\psi_n\}$ coincide with $\{\phi_n\}$, $\mathcal{J} = \{1, ..., N\}$ and $\mathcal{I} = \{N_0\}$ where N_0 is such that $\langle g, \phi_{N_0} \rangle_{L^2(D)} \neq 0$. Moreover, what is interesting, this formulation leads to a linear interpretation of the operator B in (5.2).

The parameters used in these experiments are set as

$$\alpha = 0.8,\ T = 1,\ h(t) \equiv 1,\ N = 36,\ N_0 = 1. \tag{5.3}$$

The numerical results are displayed in Figures 2 and 3, which show that the method localizes the sources well. The relative L^2 errors are collected by Table 1. Since the approximation is obtained on the basis functions ϕ_n, the discontinuities of the true source terms are not exactly recovered. This can be seen from Figure 3 and the comparison between the errors of $(e1)$ and $(e2)$.

	$\frac{\|f-f_N\|_{L^2(D)}}{\|f\|_{L^2(D)}}$	γ_f	$\frac{\|\|g\|-\|g_N\|\|_{L^2(D)}}{\|g\|_{L^2(D)}}$	γ_g
$(e1)$	6.06e-2	Not applicable	2.46e-2	Not applicable
$(e2)$	4.88e-1		5.46e-1	
$(e1a)$	2.55e-1	1e-10	1.06e-1	1e-12
$(e1b)$	2.77e-1	1e-10	7.54e-2	1e-12
$(e1c)$	3.76e-1	1e-10	1.81e-1	1e-11
$(e2a)$	5.20e-1	1e-10	8.35e-1	1e-16
$(e2b)$	6.16e-1	1e-13	6.54e-1	1e-16
$(e2c)$	6.47e-1	1e-13	1.24e-0	1e-16

Table 1: Relative L^2 errors and the regularized parameters.

5.3 Numerical results with observations on partial domain

In this subsection, we consider the numerical reconstruction with partial measurements, i.e. $D_{mea} \subset D$ and $D_{mea} \neq D$. Here $\{\psi_n\}$ are set as the characteristic functions on each uniformly partition of D_{mea} upon the polar coordinates (r, θ).

Given the noisy data $(\widehat{\mathbf{E}}^\delta, \widehat{\mathbf{C}}^\delta)$, for the first equation we set the optimization problem as

$$\arg\min_{\vec{f}_N \in \mathbb{R}^N} \left\{ \|A\vec{f}_N - \widehat{\mathbf{E}}^\delta\|_{l^2}^2 + \gamma_f \|\vec{f}_N\|_{l^2}^2 \right\}.$$

Due to the nonlinearity of the second equation, we choose the Levenberg-Marquardt type Newton's iteration

$$\vec{g}_{l+1} = \vec{g}_l + [B'(\vec{g}_l)^\top B'(\vec{g}_l) + \gamma_g I_N]^{-1} B'(\vec{g}_l)^\top (\widehat{\mathbf{C}}^\delta - B\vec{g}_l),$$

and the Frechet derivative B' of B is given as

$$B'(g)[h] = \int_0^T \mathbf{R}^\top [\mathbf{g}(\tau)\mathbf{h}(\tau)^\top + \mathbf{h}(\tau)\mathbf{g}(\tau)^\top]\mathbf{R}\ d\tau.$$

We try three kinds of subsets of D which are set as the observed area and can be seen in Figure 4. (a) is a concentric with radius $1/4$, (b) is the annulus between the circles

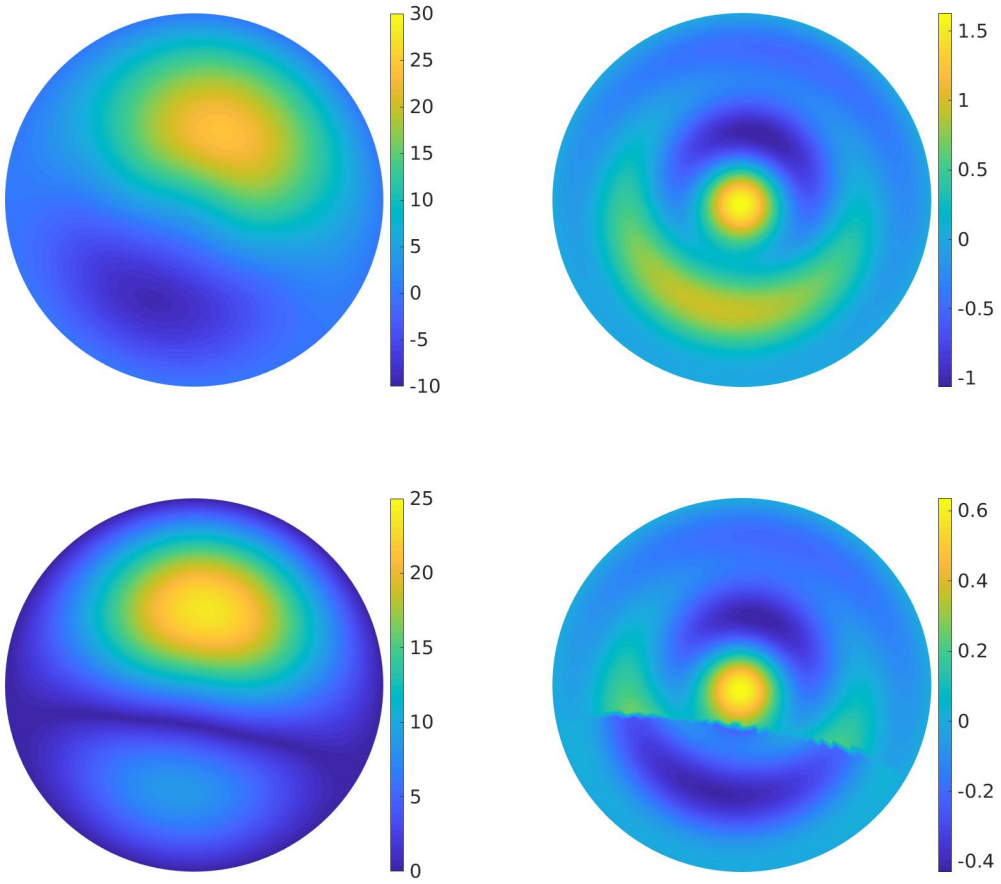

Figure 2: Experiment $(e1)$ for f (top) and $|g|$ (bottom).
Numerical approximation (left), difference between exact solution and approximation (right).

with radius $3/4$ and 1, and (c) contains two segments of the annulus in (b) with $\pi/4$ radian span. The exact solutions and the parameter setting (5.3) in experiments $(e1)$ and $(e2)$ are still used but the corresponding notations are changed to $(e1a)$, $(e1b)$, $(e1c)$ and $(e2a)$, $(e2b)$, $(e2c)$. The results are displayed in Figures 5, 6, 7, 8, and the relative L^2 errors are recorded in Table 1. In these experiments, the values of the regularized parameters γ_f, γ_g are chosen empirically.

Similar to the results of experiments $(e1)$ and $(e2)$, the reconstructions for smooth exact solutions are better than the ones for nonsmooth case. Furthermore, due to the lack of measured data, the performance of experiments $\{(e1j), (e2j) : j = a, b, c\}$ is worse than $(e1)$ and $(e2)$, and this can be seen in Figures 5, 6, 7, 8 and Table 1. Also, the results for $(e2c)$ show that the observed subdomain (c) in Figure 4 for the discontinuous case is close to the limit in terms of noise level and the size of the subdomain of which can ensure a useful localization of the source.

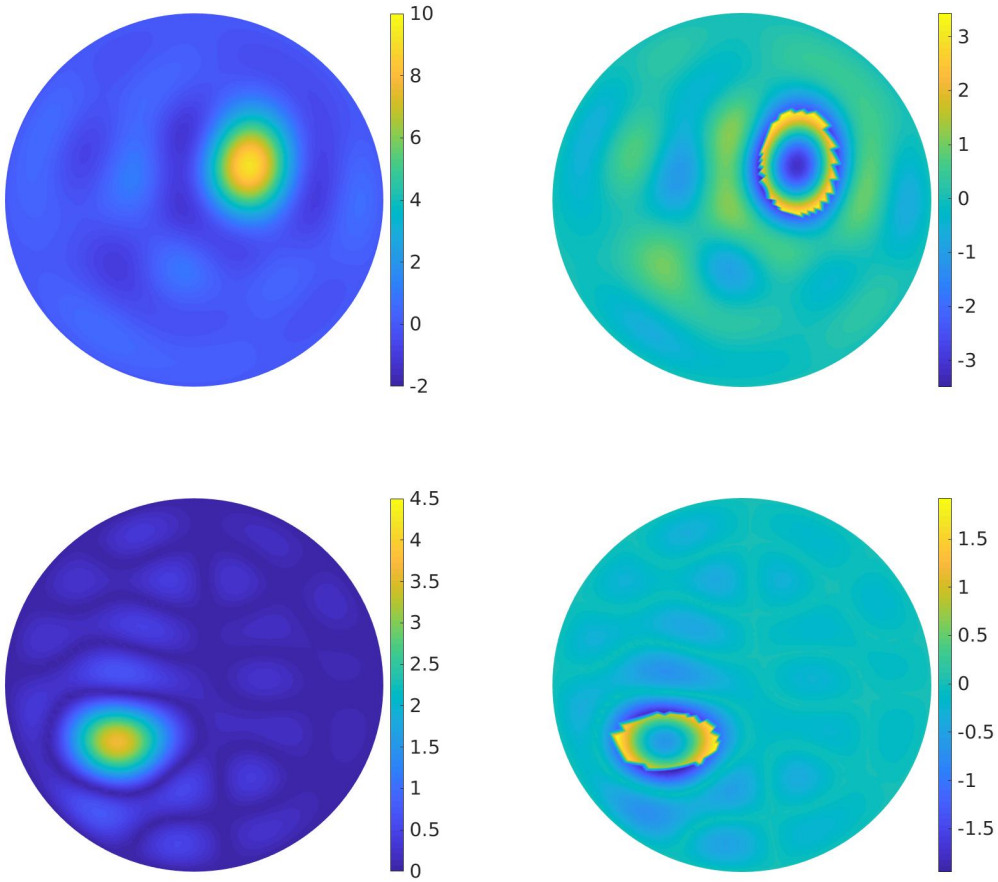

Figure 3: Experiment ($e2$) for f (top) and $|g|$ (bottom).
Numerical approximation (left), difference between exact solution and approximation (right).

Acknowledgement

PN is partially supported by China Scholarship Council and Finnish National Agency for Education (ID:201702720003), NSFC (key projects no.11331004, no.11421110002) and the Programme of Introducing Talents of Discipline to Universities (no.B08018). TH and ZZ were supported by the Three-year grant "Stochastic inverse problems in atmospheric tomography" of the University of Helsinki. In addition, TH was supported by the Academy of Finland via projects 275177 and 314879.

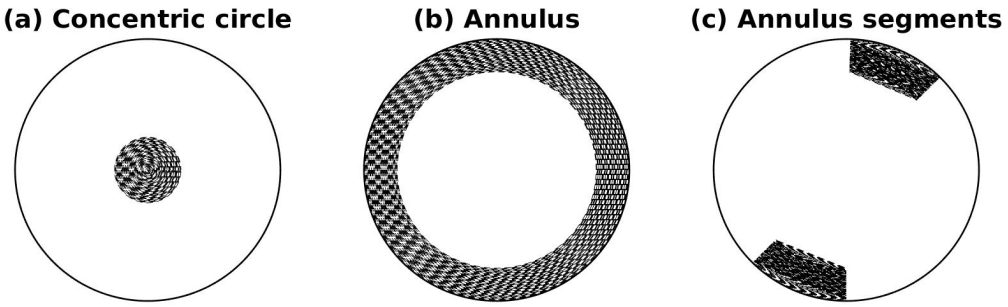

Figure 4: Three partial domains D_{mea} in section 5.3. In each case the shaded area is observed.

References

[1] E. E. Adams and L. W. Gelhar. Field study of dispersion in a heterogeneous aquifer: 2. spatial moments analysis. *Water Resources Research*, 28(12):3293–3307, 1992.

[2] G. Bao, C. Chen, and P. Li. Inverse random source scattering problems in several dimensions. *SIAM/ASA J. Uncertain. Quantif.*, 4(1):1263–1287, 2016. URL: https://doi.org/10.1137/16M1067470.

[3] G. Bao, C. Chen, and P. Li. Inverse random source scattering for elastic waves. *SIAM Journal on Numerical Analysis*, 55(6):2616–2643, 2017.

[4] G. Bao, S.-N. Chow, P. Li, and H. Zhou. Numerical solution of an inverse medium scattering problem with a stochastic source. *Inverse Problems*, 26(7):074014, 2010.

[5] G. Bao, S.-N. Chow, P. Li, and H. Zhou. An inverse random source problem for the Helmholtz equation. *Math. Comp.*, 83(285):215–233, 2014. URL: https://doi.org/10.1090/S0025-5718-2013-02730-5.

[6] E. Barkai, R. Metzler, and J. Klafter. From continuous time random walks to the fractional fokker-planck equation. *Phys. Rev. E*, 61:132–138, Jan 2000. URL: https://link.aps.org/doi/10.1103/PhysRevE.61.132, doi:10.1103/PhysRevE.61.132.

[7] B. Berkowitz, A. Cortis, M. Dentz, and H. Scher. Modeling non-fickian transport in geological formations as a continuous time random walk. *Reviews of Geophysics*, 44(2), 2006.

[8] L. Borcea, G. Papanicolaou, C. Tsogka, and J. Berryman. Imaging and time reversal in random media. *Inverse Problems*, 18(5):1247, 2002.

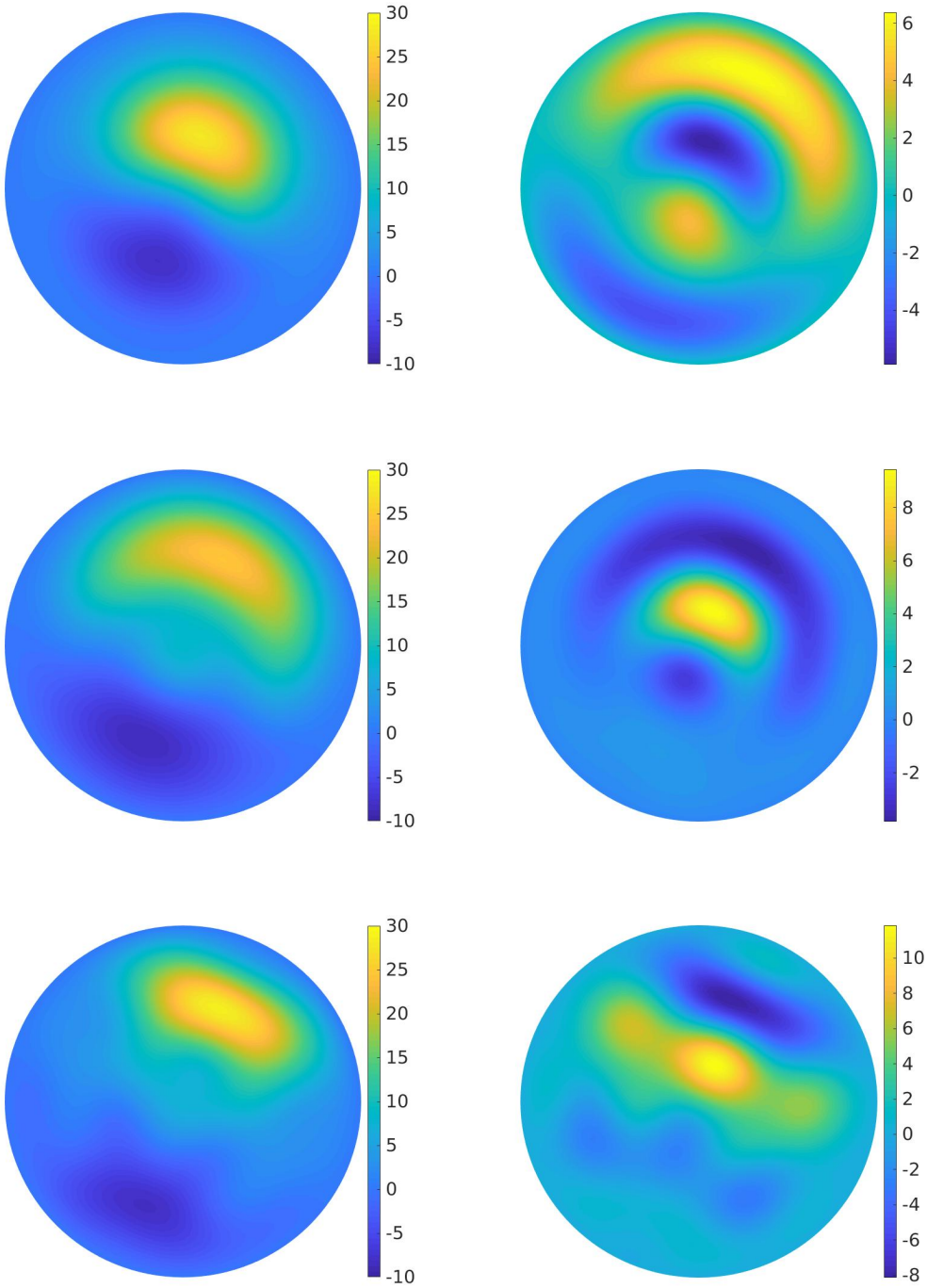

Figure 5: Reconstruction for f with experiment $(e1a)$ (top), $(e1b)$ (middle) and $(e1c)$ (bottom). Numerical approximation (left), difference between exact solution and approximation (right).

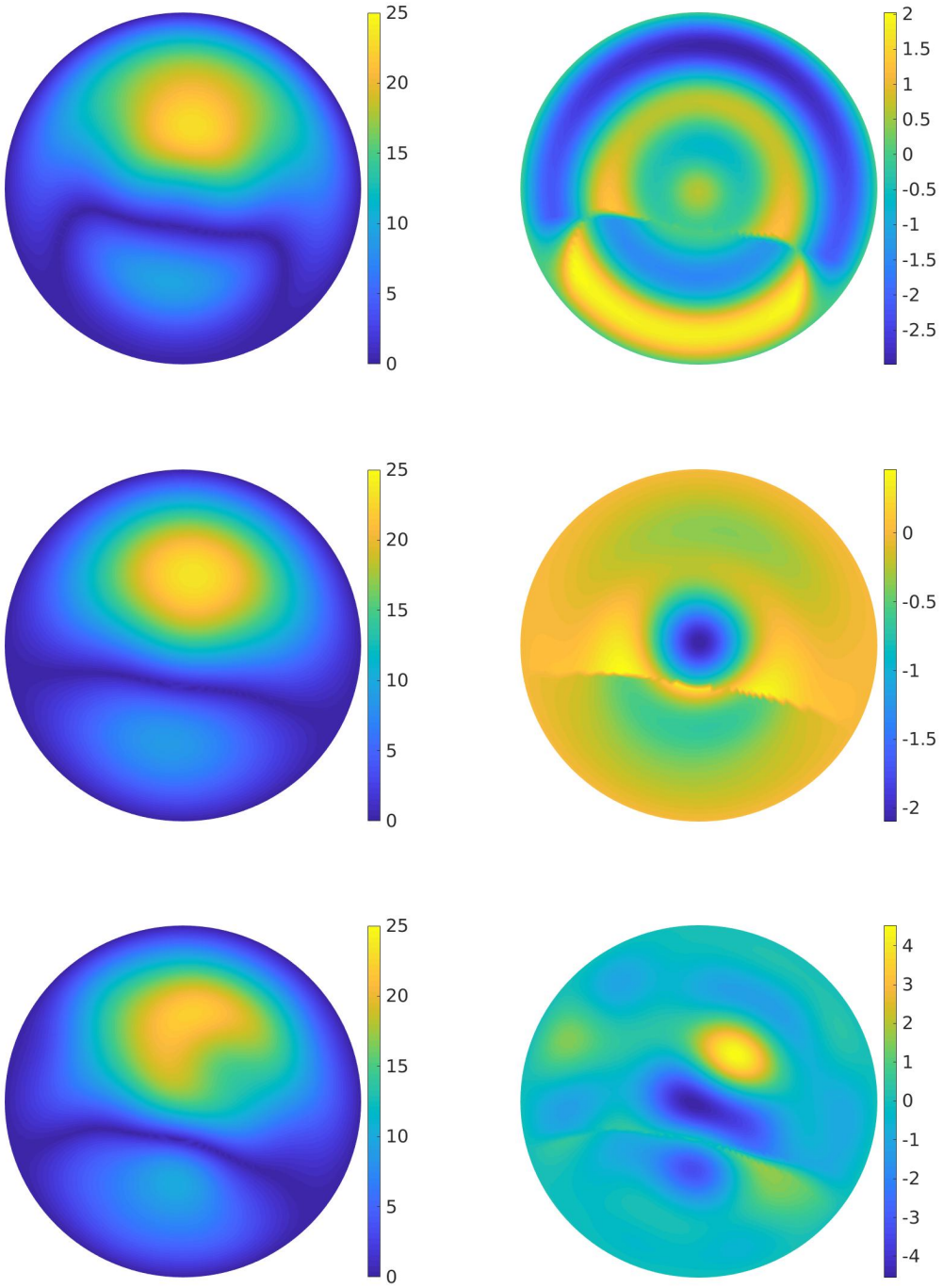

Figure 6: Reconstruction for $|g|$ with experiment $(e1a)$ (top), $(e1b)$ (middle) and $(e1c)$ (bottom). Numerical approximation (left), difference between exact solution and approximation (right).

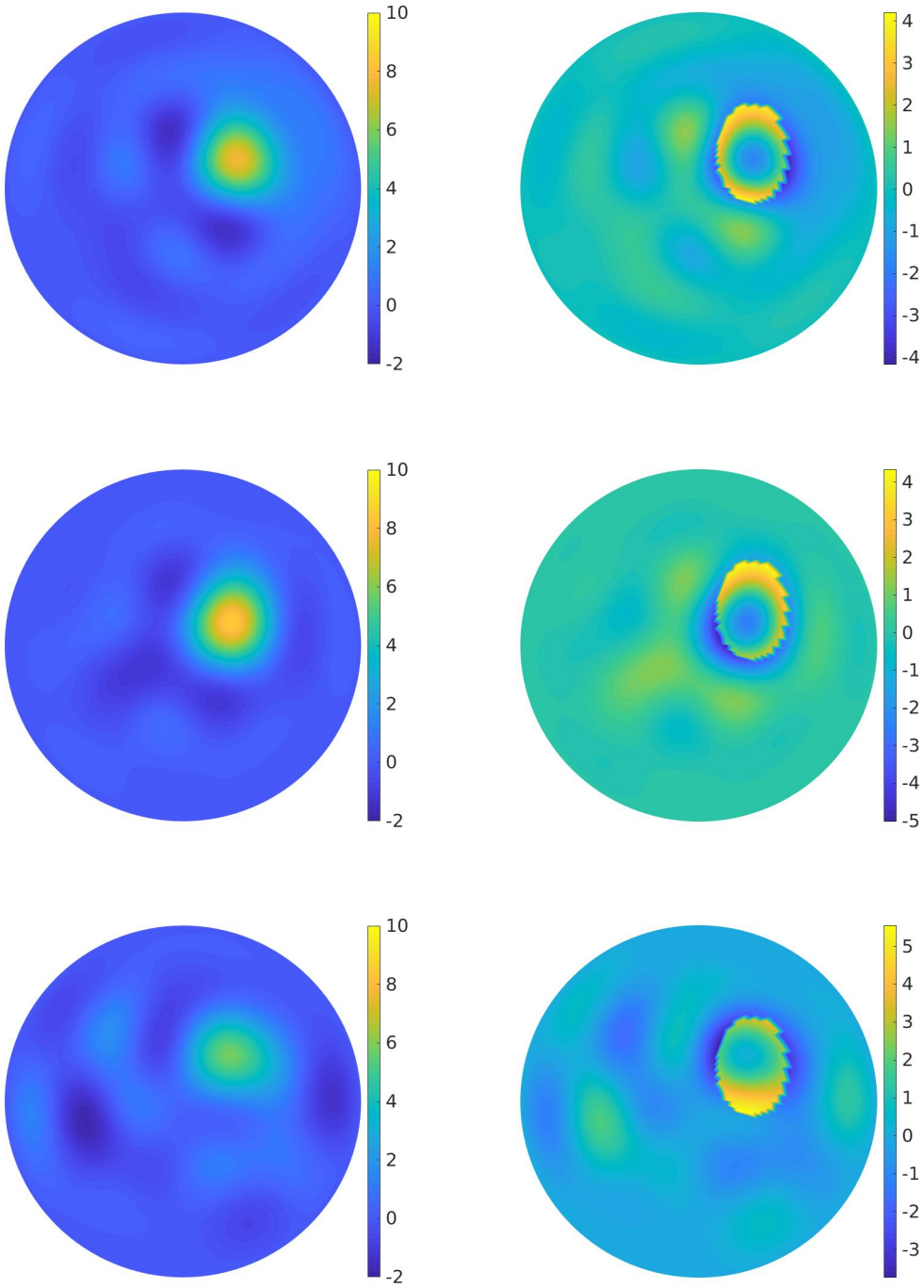

Figure 7: Reconstruction for f with experiment $(e2a)$ (top), $(e2b)$ (middle) and $(e2c)$ (bottom). Numerical approximation (left), difference between exact solution and approximation (right).

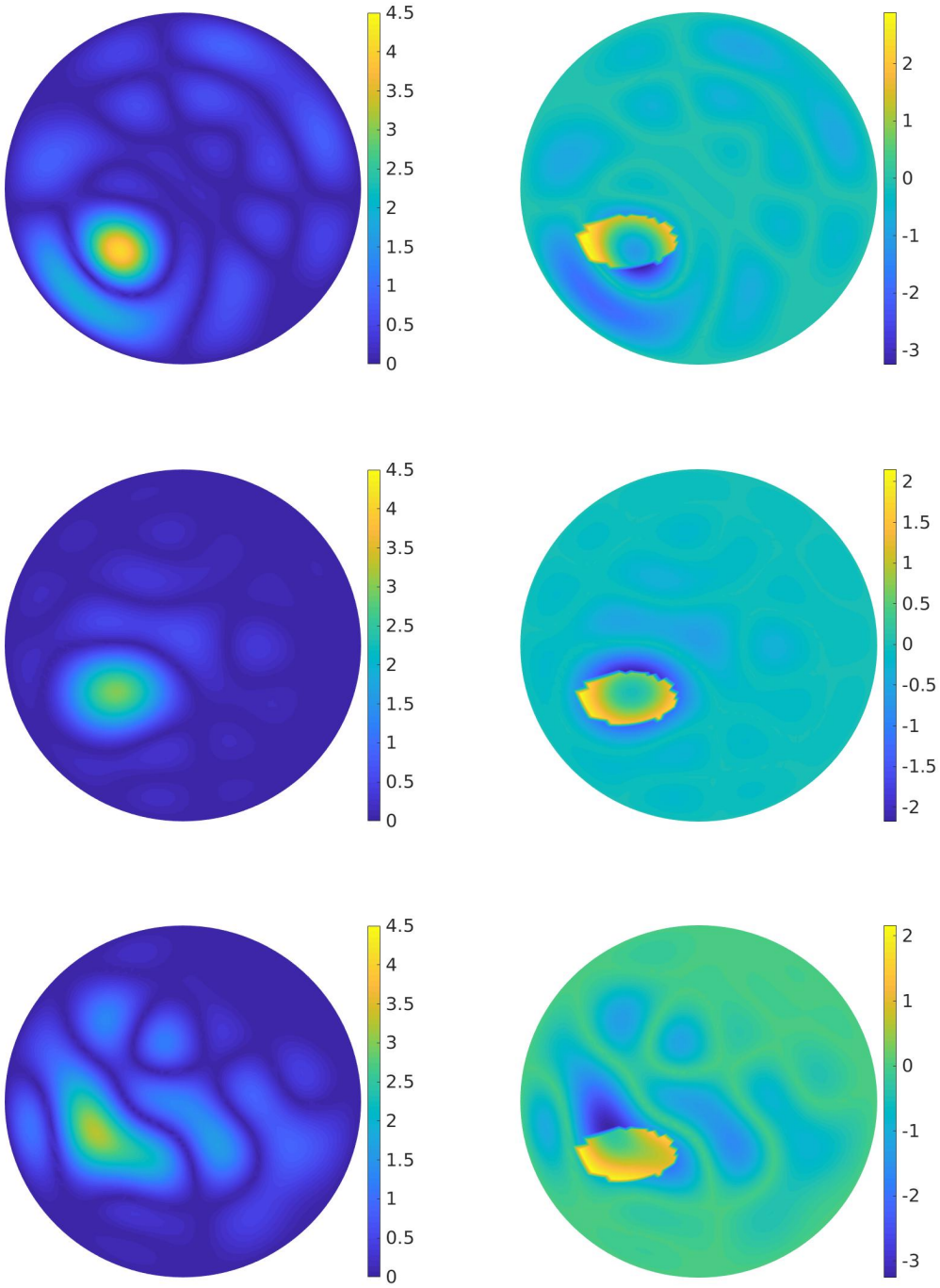

Figure 8: Reconstruction for $|g|$ with experiment $(e2a)$ (top), $(e2b)$ (middle) and $(e2c)$ (bottom). Numerical approximation (left), difference between exact solution and approximation (right).

[9] J.-P. Bouchaud and A. Georges. Anomalous diffusion in disordered media: Statistical mechanisms, models and physical applications. *Physics Reports*, 195(4):127 – 293, 1990. URL: http://www.sciencedirect.com/science/article/pii/037015739090099N, doi:https://doi.org/10.1016/0370-1573(90)90099-N.

[10] P. Caro, T. Helin, and M. Lassas. Inverse scattering for a random potential. *arXiv preprint arXiv:1605.08710*, 2016.

[11] J. Cheng, J. Nakagawa, M. Yamamoto, and T. Yamazaki. Uniqueness in an inverse problem for a one-dimensional fractional diffusion equation. *Inverse Problems*, 25(11):115002, 16, 2009. URL: http://dx.doi.org/10.1088/0266-5611/25/11/115002, doi:10.1088/0266-5611/25/11/115002.

[12] A. Devaney. The inverse problem for random sources. *Journal of Mathematical Physics*, 20(8):1687–1691, 1979.

[13] A. Einstein. Über die von der molekularkinetischen theorie der wärme geforderte bewegung von in ruhenden flüssigkeiten suspendierten teilchen. *Annalen der physik*, 322(8):549–560, 1905.

[14] M. M. El-Borai. Some probability densities and fundamental solutions of fractional evolution equations. *Chaos, Solitons & Fractals*, 14(3):433–440, 2002.

[15] J. Garnier and G. Papanicolaou. Passive sensor imaging using cross correlations of noisy signals in a scattering medium. *SIAM Journal on Imaging Sciences*, 2(2):396–437, 2009.

[16] J. Garnier and G. Papanicolaou. Correlation-based virtual source imaging in strongly scattering random media. *Inverse Problems*, 28(7):075002, 2012.

[17] J. Garnier and G. Papanicolaou. *Passive imaging with ambient noise*. Cambridge University Press, 2016.

[18] Y. Gefen, A. Aharony, and S. Alexander. Anomalous diffusion on percolating clusters. *Phys. Rev. Lett.*, 50:77–80, Jan 1983. URL: https://link.aps.org/doi/10.1103/PhysRevLett.50.77, doi:10.1103/PhysRevLett.50.77.

[19] R. Gorenflo, A. A. Kilbas, F. Mainardi, and S. V. Rogosin. *Mittag-Leffler functions, related topics and applications*. Springer Monographs in Mathematics. Springer, Heidelberg, 2014. URL: http://dx.doi.org/10.1007/978-3-662-43930-2, doi:10.1007/978-3-662-43930-2.

[20] Y. Hatano and N. Hatano. Dispersive transport of ions in column experiments: An explanation of long-tailed profiles. *Water resources research*, 34(5):1027–1033, 1998.

[21] T. Helin, S. Kindermann, J. Lehtonen, and R. Ramlau. Atmospheric turbulence profiling with unknown power spectral density. *Inverse Problems*, 2018.

[22] T. Helin, M. Lassas, L. Oksanen, and T. Saksala. Correlation based passive imaging with a white noise source. *arXiv preprint arXiv:1609.08022*, 2016.

[23] T. Helin, M. Lassas, and L. Päivärinta. Inverse acoustic scattering problem in half-space with anisotropic random impedance. *Journal of Differential Equations*, 262(4):3139–3168, 2017.

[24] B. Jin, R. Lazarov, and Z. Zhou. An analysis of the L1 scheme for the subdiffusion equation with nonsmooth data. *IMA J. Numer. Anal.*, 36(1):197–221, 2016. URL: http://dx.doi.org/10.1093/imanum/dru063, doi:10.1093/imanum/dru063.

[25] B. Jin and W. Rundell. A tutorial on inverse problems for anomalous diffusion processes. *Inverse Problems*, 31(3):035003, 40, 2015. URL: https://doi.org/10.1088/0266-5611/31/3/035003.

[26] A. A. Kilbas, H. M. Srivastava, and J. J. Trujillo. *Theory and applications of fractional differential equations*, volume 204 of *North-Holland Mathematics Studies*. Elsevier Science B.V., Amsterdam, 2006.

[27] J. Klafter and R. Silbey. Derivation of the continuous-time random-walk equation. *Phys. Rev. Lett.*, 44:55–58, Jan 1980. URL: https://link.aps.org/doi/10.1103/PhysRevLett.44.55, doi:10.1103/PhysRevLett.44.55.

[28] M. Li, C. Chen, and P. Li. Inverse random source scattering for the helmholtz equation in inhomogeneous media. *Inverse Problems*, 34(1):015003, 2017.

[29] P. Li. An inverse random source scattering problem in inhomogeneous media. *Inverse Problems*, 27(3):035004, 22, 2011. URL: https://doi.org/10.1088/0266-5611/27/3/035004.

[30] P. Li and G. Yuan. Stability on the inverse random source scattering problem for the one-dimensional helmholtz equation. *Journal of Mathematical Analysis and Applications*, 450(2):872–887, 2017.

[31] Z. Li, Y. Luchko, and M. Yamamoto. Analyticity of solutions to a distributed order time-fractional diffusion equation and its application to an inverse problem. *Comput. Math. Appl.*, 73(6):1041–1052, 2017. URL: https://doi.org/10.1016/j.camwa.2016.06.030.

[32] Y. Liu and Z. Zhang. Reconstruction of the temporal component in the source term of a (time-fractional) diffusion equation. *Journal of Physics A: Mathematical and Theoretical*, 50(30):305203, 2017. URL: http://stacks.iop.org/1751-8121/50/i=30/a=305203.

[33] Y. Luchko. Maximum principle for the generalized time-fractional diffusion equation. *J. Math. Anal. Appl.*, 351(1):218–223, 2009. URL: https://doi.org/10.1016/j.jmaa.2008.10.018.

[34] Y. Luchko. Maximum principle and its application for the time-fractional diffusion equations. *Fract. Calc. Appl. Anal.*, 14(1):110–124, 2011. URL: https://doi.org/10.2478/s13540-011-0008-6.

[35] F. Mainardi. *Fractional calculus and waves in linear viscoelasticity*. Imperial College Press, London, 2010. An introduction to mathematical models. URL: http://dx.doi.org/10.1142/9781848163300, doi:10.1142/9781848163300.

[36] R. Metzler and J. Klafter. The random walk's guide to anomalous diffusion: a fractional dynamics approach. *Physics Reports*, 339(1):1 – 77, 2000. URL: http://www.sciencedirect.com/science/article/pii/S0370157300000703, doi:https://doi.org/10.1016/S0370-1573(00)00070-3.

[37] J. B. Mijena and E. Nane. Space–time fractional stochastic partial differential equations. *Stochastic Processes and their Applications*, 125(9):3301–3326, 2015.

[38] R. Nigmatullin. The realization of the generalized transfer equation in a medium with fractal geometry. *physica status solidi (b)*, 133(1):425–430, 1986.

[39] B. Ø ksendal. *Stochastic differential equations*. Universitext. Springer-Verlag, Berlin, sixth edition, 2003. An introduction with applications. URL: https://doi.org/10.1007/978-3-642-14394-6.

[40] I. Podlubny. *Fractional differential equations*, volume 198 of *Mathematics in Science and Engineering*. Academic Press, Inc., San Diego, CA, 1999. An introduction to fractional derivatives, fractional differential equations, to methods of their solution and some of their applications.

[41] H. Pollard. The completely monotonic character of the Mittag-Leffler function $E_a(-x)$. *Bull. Amer. Math. Soc.*, 54:1115–1116, 1948. URL: http://dx.doi.org/10.1090/S0002-9904-1948-09132-7, doi:10.1090/S0002-9904-1948-09132-7.

[42] W. Rundell and Z. Zhang. Fractional diffusion: recovering the distributed fractional derivative from overposed data. *Inverse Problems*, 33(3):035008, 27, 2017. URL: https://doi.org/10.1088/1361-6420/aa573e.

[43] K. Sakamoto and M. Yamamoto. Initial value/boundary value problems for fractional diffusion-wave equations and applications to some inverse problems. *J. Math. Anal. Appl.*, 382(1):426–447, 2011. URL: http://dx.doi.org/10.1016/j.jmaa.2011.04.058, doi:10.1016/j.jmaa.2011.04.058.

[44] R. Sakthivel, S. Suganya, and S. M. Anthoni. Approximate controllability of fractional stochastic evolution equations. *Computers & Mathematics with Applications*, 63(3):660–668, 2012.

[45] N. H. Tuan and E. Nane. Inverse source problem for time-fractional diffusion with discrete random noise. *Statistics & Probability Letters*, 120:126–134, 2017.

[46] A. W. Wharmby and R. L. Bagley. Generalization of a theoretical basis for the application of fractional calculus to viscoelasticity. *Journal of Rheology (1978-present)*, 57(5):1429–1440, 2013.

[47] A. W. Wharmby and R. L. Bagley. Modifying maxwell's equations for dielectric materials based on techniques from viscoelasticity and concepts from fractional calculus. *International Journal of Engineering Science*, 79:59–80, 2014.

[48] G.-a. Zou. A galerkin finite element method for time-fractional stochastic heat equation. *arXiv preprint arXiv:1612.02082*, 2016.